



DCCA multi cross-correlation analysis applied on EEG signals to study motor activity (Real/Imaginary)

Fernando Ferraz Ribeiro ^{a,b,c}, Andréa de Almeida Brito ^d, Florêncio Mendes Oliveira Filho ^{a,c}, Juan Alberto Leyva Cruz ^e, Gilney Figueira Zebende ^e,*
 *Earth Sciences and Environment Modeling Program, State University of Feira de Santana, Bahia, Brazil
^bFederal University of Bahia, Salvador, Brazil
^cSENAI CIMATEC University Center, Salvador, Bahia, Brazil
^dFederal Institute of Education, Science and Technology, Salvador, Bahia, Brazil
^eState University of Feira de Santana, Bahia, Brazil

ARTICLE INFO

Keywords:
 DFA
 DCCA
 DCCA multiple cross-correlation coefficient
 EEG signals
 Brain

ABSTRACT

We applied the DCCA multiple cross-correlation coefficient to analyze time series of EEG experiment, where 109 subjects performed four tasks involving real and imaginary motor activities. In this case, four specific channels were selected on the scalp: two on the frontal and two on parietal region. As a result, the DCCA multiple cross-correlation coefficient identified that there is a single signature for each subject. Globally, there is no significant difference between the real and the imaginary task. The frontal channels had greater multiple cross-correlation values than the parietal ones, especially for time scales around 0.42s, and with smaller standard deviations. According to our results, the proposal to study multiple time series at the same time by using the DCCA multiple cross-correlation coefficient is feasible and robust for EEG analysis. Finally, the coefficient was applied in a substantial number of subjects, tasks, and experiments producing high-quality results (figures, movies, and tables), and this study will probably kick off of a new approach to analyzing multiple cross-correlations in EEG signals.

1. Introduction

An electroencephalogram, or EEG, is a test that evaluates the electrical activity of the brain. It is normally a non-invasive method, where tiny electrodes are placed on the scalp to track brain wave patterns and send them to a computer. The EEG equipment measures the electric potential difference (usually in μ V) between each of the 64 electrodes and a reference electrode, usually placed in the ear lobe. These impulses are amplified and recorded over time, generating time series for each sensor (with high temporal resolution and low spatial resolution). The international 10 – 10 system was used to map the positions, where 64 electrodes were fixed in the experiments, that collected the data used in this analysis. The nomenclature of the channels in this system is given according to the region in which they are located, namely *F* (frontal), *T* (temporal), *C* (central), *P* (parietal), and *O* (occipital). Channels located on the midline are indexed by the letter *z* (zero), channels located on the left side are represented by odd indexes, and those on the right side are represented by even indexes (see Fig. 1). EEG analysis is useful for diagnosing problems such as epilepsy, dementia, sleep disorders, and other health problems. The diagnosis

normally focuses on the spectral content of the EEG and on the type of neural oscillations (or brain waves) that can be observed in these signals. Most observed signals are between 1 and 20 Hz. Although EEG is almost a centenary technique, in recent decades, it has addressed new problems, such as brain-triggered neuro-rehabilitation treatments, experimental psychology, or even computational neuroscience, due to its versatility and accessibility, alongside the advances in signal processing [1,2] that enhance the analysis possibilities in the field. Some new techniques for analyzing EEG signals that we wish to highlight are the root mean square fluctuation function, F_{DFA} , studying brain activity in the reading task [3,4], the quantification of long-range correlation of EEG signals [5], and recently in the statistical study of the EEG cross-correlation of two signals using the detrended cross-correlation [6].

In this paper, we will analyze multiple time series of EEG signals produced in a motor activity (Real/Imaginary) by 109 subjects via the Detrended Multiple Cross-Correlation Coefficient [7]. Based on symmetry criteria, we chose the channels *F*₃, *F*₆, *P*₃, and *P*₆ to apply this new statistical tool. In the sections below we present the Data and

* Corresponding author.

E-mail address: gfzebende@uefs.br (G.F. Zebende).

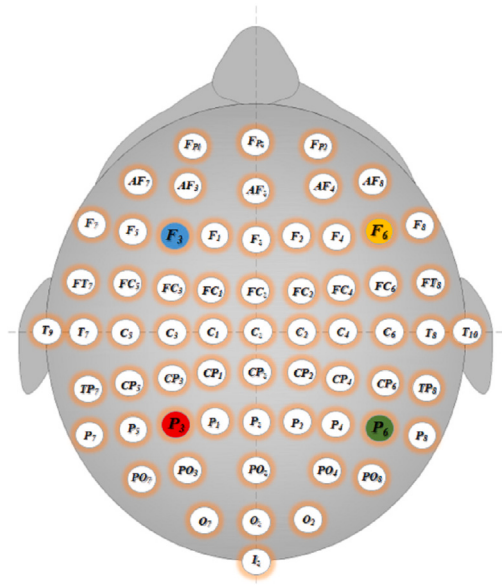


Fig. 1. Electrode positions based on international 10–10 system for 64 channels. The circles F_3 (blue), F_6 (yellow), P_3 (red), and P_6 (green) identify the channels used for multiple cross-correlation analysis.

Method with dataset, methodology, and calculations used to analyze the data, including pre-processing strategies. Afterward, we present the **Results** with its statistics and a discussion and, finally we make a **Conclusion**.

2. Data and method

Data

The EEG files were downloaded from the *Physionet* open-access website, available at this link:

<https://physionet.org/content/eegmmidb/1.0.0/>

Physionet operates under the Open Data Commons Attribution License (ODC-By) v1.0. This website presents a large quantity/quality of EEG experiments, in EDF (European Data Format) format, computed by a Brain-Computer Interface Technology, BCI-2000 [8], on the premise of the international 10–10 system. The *Physionet* website was accessed on January 11, 2022 for this study, taking into account that we did not have any information that could identify individual participants. These EEG signals were performed in 14 experiments on a population of 109 subjects with the objective of record brain signals during various motor stimuli, or tasks, briefly described below.

The first two activities were baseline references: in the first, the subjects were resting with eyes opened, and in the second, with eyes closed (one minute for each). The other four activities (task) were a combination of two categories with two possible options each. In general, the experiments consisted of making the subjects react to a visual stimuli, in other words, a target that appears on a screen. One category is about the target position, i.e., one option was a target appearing on the **Left/Right** of the screen, and the other was a target appearing on the **Top/Down**. The second category determined if the subject actually executed a body movement related to the target position (**Real**) or if the corresponding action was just imagined (**Imaginary**). All experiments for these 109 subjects were downloaded, but we have decided to delete the EEG relating to S106, because the experiment 5 (Top/Down Real - task 3) for this subject have only $N = 5808$ values.

These tasks, with approximately two minutes of duration, are better summarized in the **Table 1**, were each task was performed three times (experiments). After introducing our database, we will describe the methodology applied for multiple cross-correlation analysis.

DCCA multiple cross-correlation methodology

The coefficient DMC_x^2 is a new statistical tool to analyze non-stationary time series in multiple applications [7]. It starts with the DFA method [9], which was proposed to identify self-affinity in a single time series, and its generalization, the DCCA method [10], for study cross-correlation in two time series. Some applications in EEG signals, of DFA and DCCA method, can be seen to analyses brain disorder, as in different physiological and pathological states of epilepsy EEG signals [11], Alzheimer disease patients [12], among other [4–6]. Specifically, DMC_x^2 is a generalization of the detrended cross-correlation coefficient, ρ_{X_a, X_b} [13] (widely known as a robust statistical tool [14]). DMC_x^2 calculates the multiple cross-correlation of one time series $\{Y\}$ (dependent variable) in relation to a number k of others time series $\{X_1\}, \{X_2\}, \{X_3\}, \dots, \{X_k\}$ (independent variable). DCCA multiple cross-correlation is defined as:

$$DMC_x^2(n) \equiv \rho_{Y, X_i}(n)^T \times \rho^{-1}(n) \times \rho_{Y, X_i}(n) \quad (1)$$

This coefficient, $0 \leq DMC_x^2(n) \leq 1$, where 0 (1), the weaker (stronger) is the relationship between the dependent and independent variables. The term $\rho^{-1}(n)$, in the Eq. (1), represent the inverse matrix of all possible combinations of ρ_{X_a, X_b} (between the independent variables); in other words:

$$\rho^{-1}(n) = \begin{pmatrix} 1 & \rho_{X_1, X_2}(n) & \rho_{X_1, X_3}(n) & \dots & \rho_{X_1, X_k}(n) \\ \rho_{X_2, X_1}(n) & 1 & \rho_{X_2, X_3}(n) & \dots & \rho_{X_2, X_k}(n) \\ \vdots & \vdots & \vdots & \ddots & \vdots \\ \rho_{X_k, X_1}(n) & \rho_{X_k, X_2}(n) & \rho_{X_k, X_3}(n) & \dots & 1 \end{pmatrix}^{-1} \quad (2)$$

In this equation, $\rho_{Y, X_i}(n)$ represent the vector of the detrended cross-correlation between the predictor variables (independent) and the target variable (dependent), and $\rho_{Y, X_i}(n)^T$ it is the transposed.

DMC_x^2 has been applied in many problems, specifically for three time series analysis, i.e., one $\{Y\}$ (dependent) and two $\{X_1\}, \{X_2\}$ (independent). Examples of these applications can be found applied to study meteorological variables [15], in statistical test [16], with the implementation of sliding windows [17], to measure the contagion effect on stock market indexes [18], to take the statistical analysis between stock market indexes [19], among other applications.

However, for the particular case of four time series, i.e., one $\{Y\}$ (dependent variable) and three $\{X_1\}, \{X_2\}, \{X_3\}$ (independent variables), there is still no cases. In this sense, from Eq. (1), the calculus of the DMC_x^2 with three independent variables can be represented by:

$$\begin{aligned} DMC_x^2 = & \left(\rho_{X_2, X_3}^2 \times \rho_{Y, X_1}^2 - \rho_{Y, X_1}^2 + \rho_{X_1, X_3}^2 \times \rho_{Y, X_2}^2 - \rho_{Y, X_2}^2 \right. \\ & + 2 \times \rho_{X_1, X_2} \times \rho_{Y, X_1} \times \rho_{Y, X_2} - 2 \times \rho_{X_1, X_3} \times \rho_{X_2, X_3} \times \rho_{Y, X_1} \\ & + \rho_{X_1, X_2}^2 \times \rho_{Y, X_3}^2 - \rho_{Y, X_3}^2 + 2 \times \rho_{X_1, X_3} \times \rho_{Y, X_1} \times \rho_{Y, X_3} \\ & - 2 \times \rho_{X_1, X_2} \times \rho_{X_2, X_3} \times \rho_{Y, X_1} \times \rho_{Y, X_3} \\ & - 2 \times \rho_{X_1, X_2} \times \rho_{X_1, X_3} \times \rho_{Y, X_2} \times \rho_{Y, X_3} \\ & + 2 \times \rho_{X_2, X_3} \times \rho_{Y, X_2} \times \rho_{Y, X_3} \Big) / \\ & \left(\rho_{X_1, X_2}^2 + \rho_{X_1, X_3}^2 + \rho_{X_2, X_3}^2 - 2 \times \rho_{X_1, X_2} \times \rho_{X_1, X_3} \times \rho_{X_2, X_3}^{-1} \right) \end{aligned} \quad (3)$$

The following section presents the data mining and its calculations for the aforementioned case.

Data mining and calculations

The data mining followed the steps presented below. In EEG experiments, usually, the end of each recording is filled with a sequence of zeros, corresponding to the time gap between the EEG machine and the recording system shutting down. In the pre-processing stage, these sequences of zeros were cut. To properly apply the DMC_x^2 and make valid comparisons between subjects and experiments, the time

Table 1

The activity executed and the experiment number for two one-minute baseline runs (one with eyes open, one with eyes closed) and three two-minute runs of a particular task.

Activity\Experiment	1	2	3	4	5	6	7	8	9	10	11	12	13	14
Baseline 1 (eyes open)	0													
Baseline 2 (eyes closed)		0												
task 1: Real (L/R)			X				X				X			
task 2: Imag (L/R)				X				X				X		
task 3: Real (T/D)					X			X					X	
task 4: Imag (T/D)						X			X					X

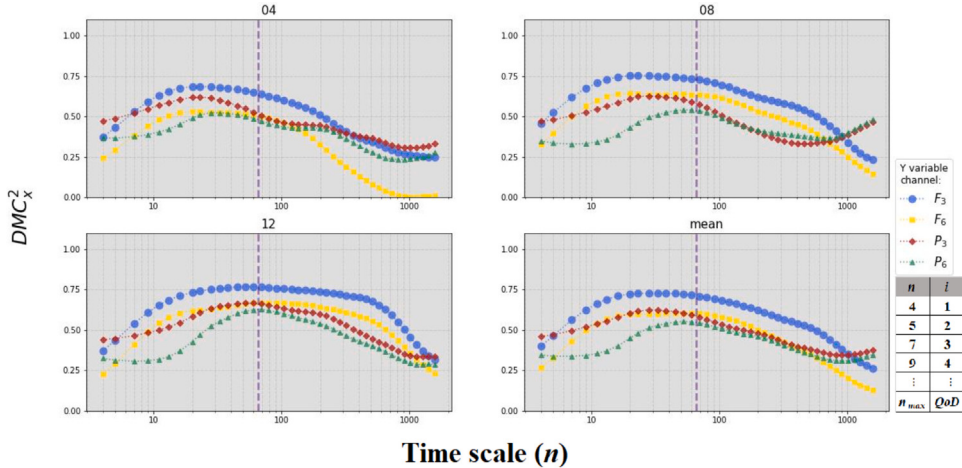


Fig. 2. DMC_x^2 as a function of time scale n . These are the results for S014 subject recordings for task 2, presenting experiments 04, 08, and 12 (Table 1) and the mean values for these experiments. The vertical line represents $n = 67$, and QoD is the total amount of time scales involved in DMC_x^2 calculations.

series must have approximately the same length N . This data mining results in 108 subjects, each performing four tasks, in three consecutive experiments (see Table 1). After, the DMC_x^2 calculation was performed, with all possible combinations between the four time series (our case of study). Due to the number of subjects, tasks, and experiments, we have a great number of results, which can be seen initially by accessing our public repository, through the link:

https://255ribeiro.github.io/Multi_Cross-correlation_EEG/

Basically, we observe the value of DMC_x^2 as a function of n for each subject, in a given task, by experiments.

For a better understanding of these results, we define a color code to denote the dependent variable used in the applied channels: F_3 (blue), F_6 (yellow), P_3 (red), and P_6 (green) (see Fig. 1). Table 2 summarize this color code, relating to the channel as the dependent variable (Y) and the ones used as the independent variables (X). As an example of this application, we randomly selected the S014 subject, to present the first results. Fig. 2 shown the value of $DMC_x^2 \times n$ for S014 subject carrying out the task 2, that is, Imaginary (Left/Righ) motor activity with: 04, 08, 12 experiments, and the mean value. In this case, the F_3 channel as a Y variable, had the highest DCCA multiple cross-correlation value, corroborating with [3] for auto-correlation analysis. The complete analysis of the results and their discussion will be presented below, in Section 3.

3. Results and discussion

As a better way to compare the stimuli in response to the motor activities, we choose a sample of five randomly subjects: S014, S036, S039, S078, and S099. Therefore, with the mean value of DMC_x^2 as a function of n , the initial results are presented as listed below:

– S014 in Fig. 3;

Table 2

The $Y[\text{Channel}]$ (dependent variable) is represented by a specific color that will be implemented in all figures with the DCCA multiple cross-correlation coefficient.

Color	$Y[\text{Channel}]$	$X[\text{Channel}1, \text{Channel}2, \text{Channel}3]$
Blue	$Y[F_3]$	$X[F_6, P_3, P_6]$
Yellow	$Y[F_6]$	$X[F_3, P_3, P_6]$
Red	$Y[P_3]$	$X[F_3, F_6, P_6]$
Green	$Y[P_6]$	$X[F_3, F_6, P_3]$

- S036 in Fig. 4;
- S039 in Fig. 5;
- S078 in Fig. 6;
- S099 in Fig. 7.

The F_3 channel as a Y variable, has in general the greatest values for $\langle DMC_x^2 \rangle$, and the task Top/Down Real and Imaginary are very similar. Also, Fig. 4 shows that the channel F_3 with the greatest DCCA multiple cross-correlation values, if compared with the channels F_6 , P_3 , and P_6 . In this case, S036 subject present a distinct behavior in relation to the S014 subject. The Fig. 5, for the S039 subject, show that for small time scale, $n \leq 10$, the parietal channels, P_3 and P_6 , as a Y variable have values for $\langle DMC_x^2 \rangle$ higher if compared to the front channels, F_3 and F_6 . The results presented in Fig. 6, the values of $\langle DMC_x^2 \rangle$ are very similar for all tasks, with its values increasing until $n = 67$. Finishing this small sample, in Fig. 7 we present the results for S099 subject. In this figure it is clear that this subject has a global behavior, in terms of $\langle DMC_x^2 \rangle$, different from the previous subjects, thus identifying a possible signature in the EEG stimulus/response measurement, when performing these four tasks (Real/Imaginary or Top/Down).

Next, for a complete visualization of this motor activity (Real/Imaginary) which confirms our assumptions, we created one on-line

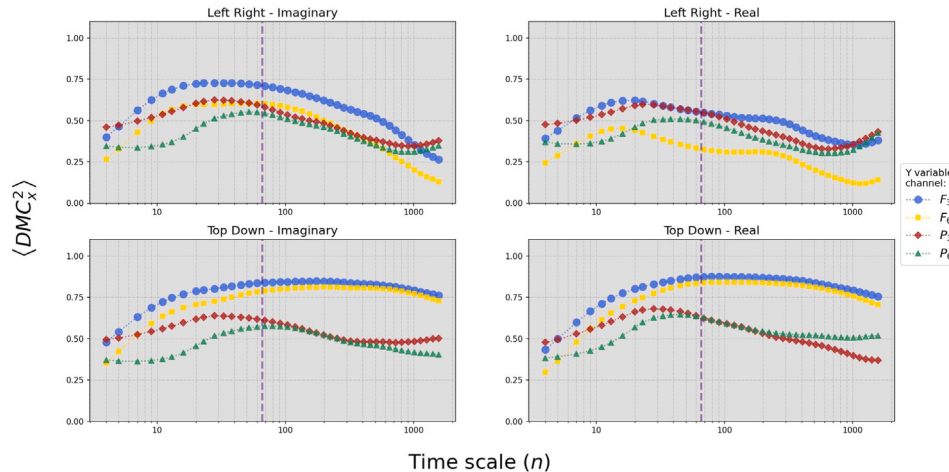


Fig. 3. Mean values of $DMC_x^2 \times n$ for all tasks: Left/Right (Imaginary), Left/Right (Real), Top/Down (Imaginary), and Top/Down (Real) for S014 subject.

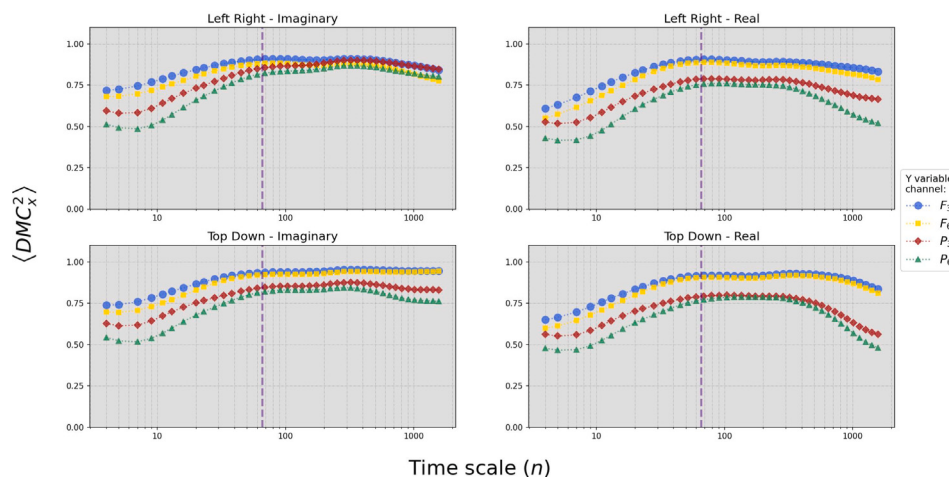


Fig. 4. Mean values of $DMC_x^2 \times n$ for all tasks: Left/Right (Imaginary), Left/Right (Real), Top/Down (Imaginary), and Top/Down (Real) for S036 subject.

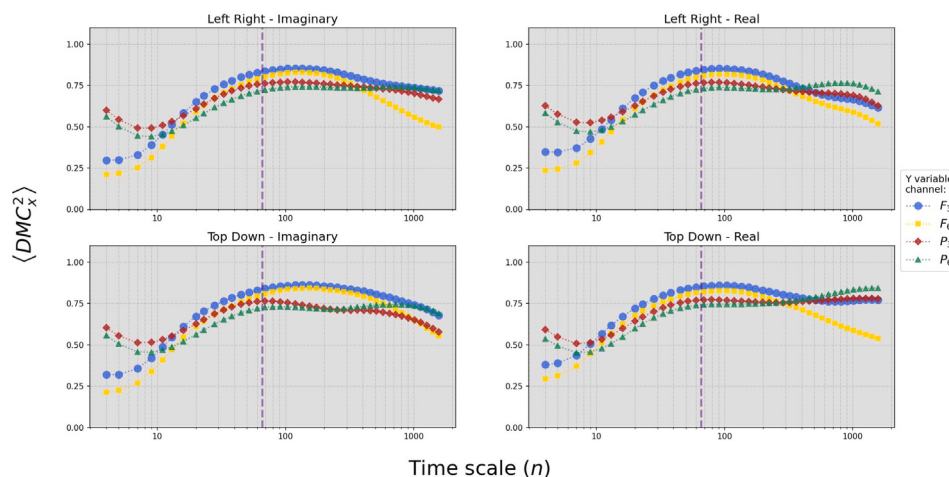


Fig. 5. Mean values of $DMC_x^2 \times n$ for all tasks: Left/Right (Imaginary), Left/Right (Real), Top/Down (Imaginary), and Top/Down (Real) for S039 subject.

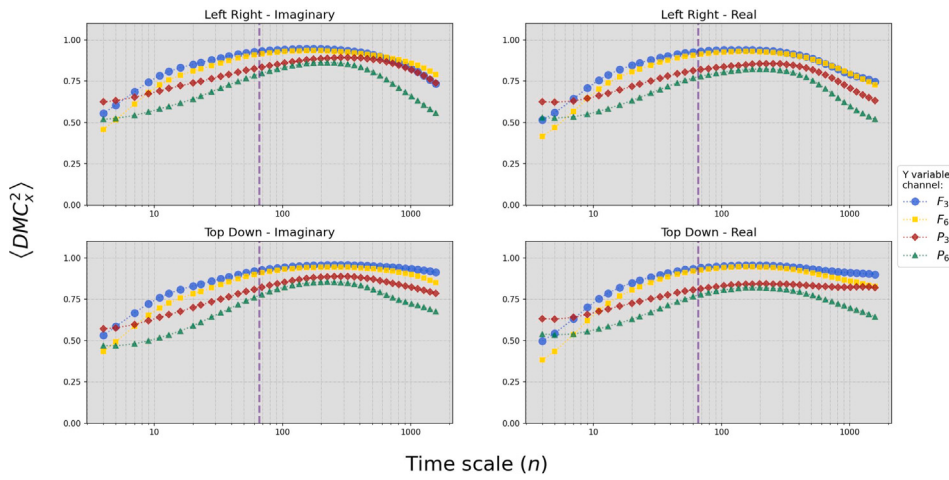


Fig. 6. Mean values of $DMC_x^2 \times n$ for all tasks: Left/Right (Imaginary), Left/Right (Real), Top/Down (Imaginary), and Top/Down (Real) for S078 subject.

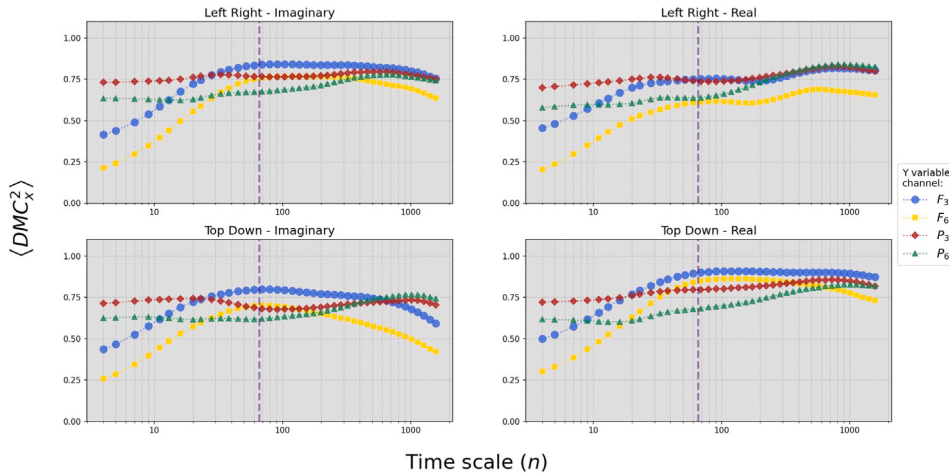


Fig. 7. Mean values of $DMC_x^2 \times n$ for all tasks: Left/Right (Imaginary), Left/Right (Real), Top/Down (Imaginary), and Top/Down (Real) for S099 subject.

public repository with $\langle DMC_x^2 \rangle$ for all subjects (with figures and videos), available at this link:

https://255ribeiro.github.io/Multi_Cross-correlation_EEG/web_report/web_site/subject_mean.html

Our public repository is very complete, for example, we can also see the difference between the Real/Imaginary task in terms of the DCCA multiple cross-correlation coefficient, for each subject j , that is:

$$diff(i-r)_j(n) \equiv \left\langle DMC_{x \text{ imaginary}}^2 \right\rangle_j(n) - \left\langle DMC_{x \text{ real}}^2 \right\rangle_j(n) \quad (4)$$

To visualize the difference between real actions and imagining the same action, a set of graphics was developed where the imaginary task of a top-down and left-right $\left\langle DMC_{x \text{ imaginary}}^2 \right\rangle_j$ action are subtracted from the real value of the same action for every subject j (Eq. (4)). See this description at the link:

https://255ribeiro.github.io/Multi_Cross-correlation_EEG/web_report/web_site/diff_ir.html

The values of $diff(i-r)_j$ are small, denoting that, the application of the DMC_x^2 is equivalent for imaginary and real case, mainly for $n \leq 67$. Following our analyses, we also calculated the global mean for DCCA multiple cross-correlation, with 108 subjects:

$$\overline{\langle DMC_x^2 \rangle}(n) = \frac{1}{108} \sum_{i=1}^{108} \langle DMC_x^2 \rangle_i(n) \quad (5)$$

See Fig. 8, were $\overline{\langle DMC_x^2 \rangle}$ is plotting as a function of n . In this figure we can see no appreciable differences between these four tasks (Left/Right and Real/Imaginary). The channel F_3 (Y) (blue circles), presents the greatest value for DCCA multiple cross-correlation coefficient, mainly around $n = 67$ or $0.42s$ (~ 2.38 Hz). It is known that, the most characteristic signals observed on EEG signal are between 1 and 20 Hz.

To investigate the dispersion in global mean, the standard deviation sd of $\langle DMC_x^2 \rangle$ for all 108 subject was calculated. The results are shown in Fig. 9. It can be seen that the sd is maximum for the channel F_6 (yellow circles), more noticeable on time scales smaller than $n = 67$ (minimum value).

The value of $\overline{\langle DMC_x^2 \rangle}$ is of great importance, because we have it calculated for a great set of subjects. Thus, we can assess how much each subject (j) deviates in relation to this global value, highlighting your individual pattern in relation to the aforementioned value, that is, through the equation

$$diff_j(n) \equiv \langle DMC_x^2 \rangle_j(n) - \overline{\langle DMC_x^2 \rangle}(n) \quad (6)$$

To corroborate with this calculation, a complete collection of figures containing the differences between each subject (j) and its global mean are available at the link:

https://255ribeiro.github.io/Multi_Cross-correlation_EEG/web_report/web_site/diff_mean.html

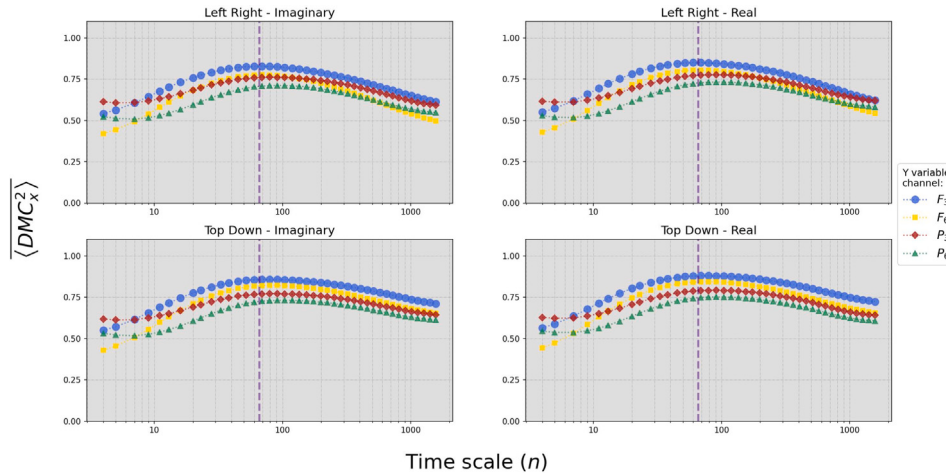


Fig. 8. $\langle DMC_x^2 \rangle \times n$ global mean for all Subjects and task (Left/Right and Real/Imaginary).

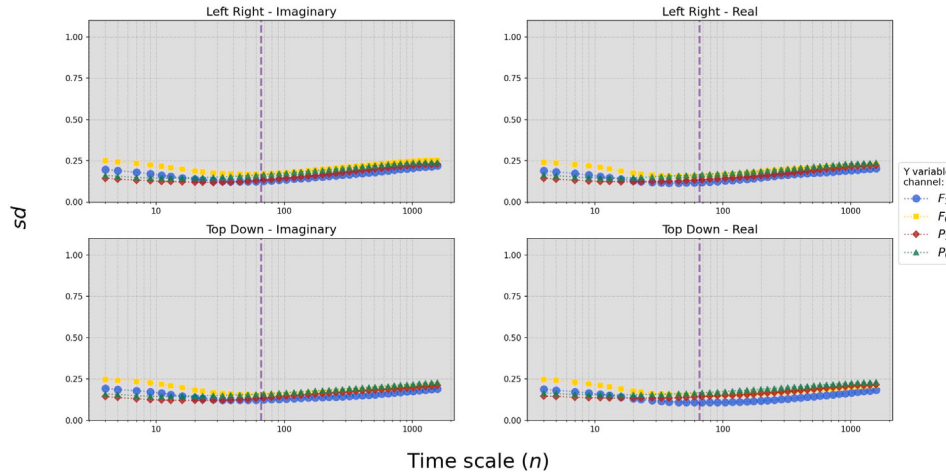


Fig. 9. sd (standard deviation) of $\langle DMC_x^2 \rangle$ for all Subjects and task.

Looking at the $diff_j(n)$, we clearly see individual patterns, that can be compared with the global mean pattern (now our reference), in the sense for example, to identify in this subject neurological abnormalities in this stimulus/response motor activity. Another way to identify individual patterns based on an average value, can be through by the mean square error function, MSE , therefore, for each subject j this function can be written by:

$$MSE(j) = \frac{1}{QoD} \sum_{i=1}^{QoD} \left(\langle DMC_x^2 \rangle [i] - \overline{\langle DMC_x^2 \rangle} [i] \right)^2 \quad (7)$$

Where QoD is the total amount of time scales used ($QoD = 42$ in this paper, see insert in Fig. 2 as an example). The results for $MSE(j)$ per channel (F_3 , F_6 , P_3 , and P_6) and task can be seeing in the Figs. 10, 11, 12, and 13.

These figures show how much each subject deviate about the global mean, by channel and task. In this sense, those subjects with the highest MSE values are those who deserve a more detailed study.

4. Conclusion

This paper proposes one statistical tool to study EEG signals in a motor activity, with the application of the DCCA multiple cross-correlation

coefficient taking into account a complete set of 108 subjects in four tasks (Real/Imaginary). In this case, the international 10 – 10 system was used and four specific channels were selected (F_3 , F_6 , P_3 , and P_6). As a result, the DCCA multiple cross-correlation coefficient identified that, there is a single signature for each subject and this visual stimulus/response presents a particular behavior as a fingerprint. Globally for these 108 subject, there is no significant difference between the imaginary and the real task. The frontal channels (F_3 and F_6) commonly had greater DCCA multiple cross-correlation values than the parietal ones (P_3 and P_6), especially for time scales around $n = 66$ (0.42 s or 2.38 Hz) where there is a smaller standard deviations. Finally, according with our results, the proposal of study multiple time series at the same time using the DCCA detrended multiple cross-correlation coefficient is feasible and robust for EEG analysis. The advantage of this method in relation to the others, in frequency domain, is that DMC_x^2 works directly in time-scale. This new coefficient is robust to analyze non-stationary time-series in multiple EEG channels. We have as a novelty the quantification of the multiple cross-correlations of each subject for a large range of time-scales, in a significant sample. As a final result, we obtained a global mean and the individual differences, as well the mean squared errors for each subject (listed in this paper as figures for each channel). This study probably will be the kick-off of a new approach to analyzing multiple cross-correlations in EEG signals.

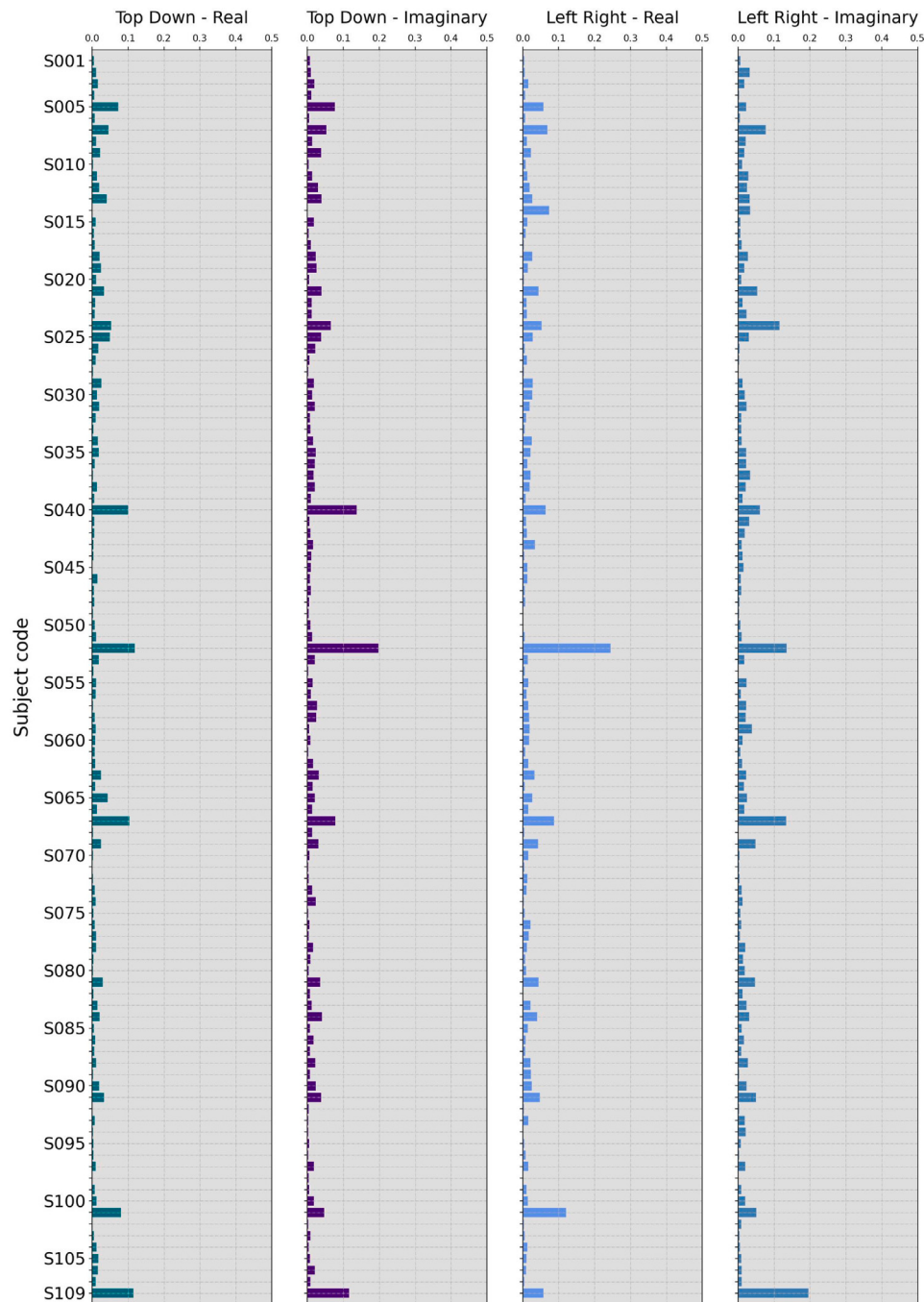
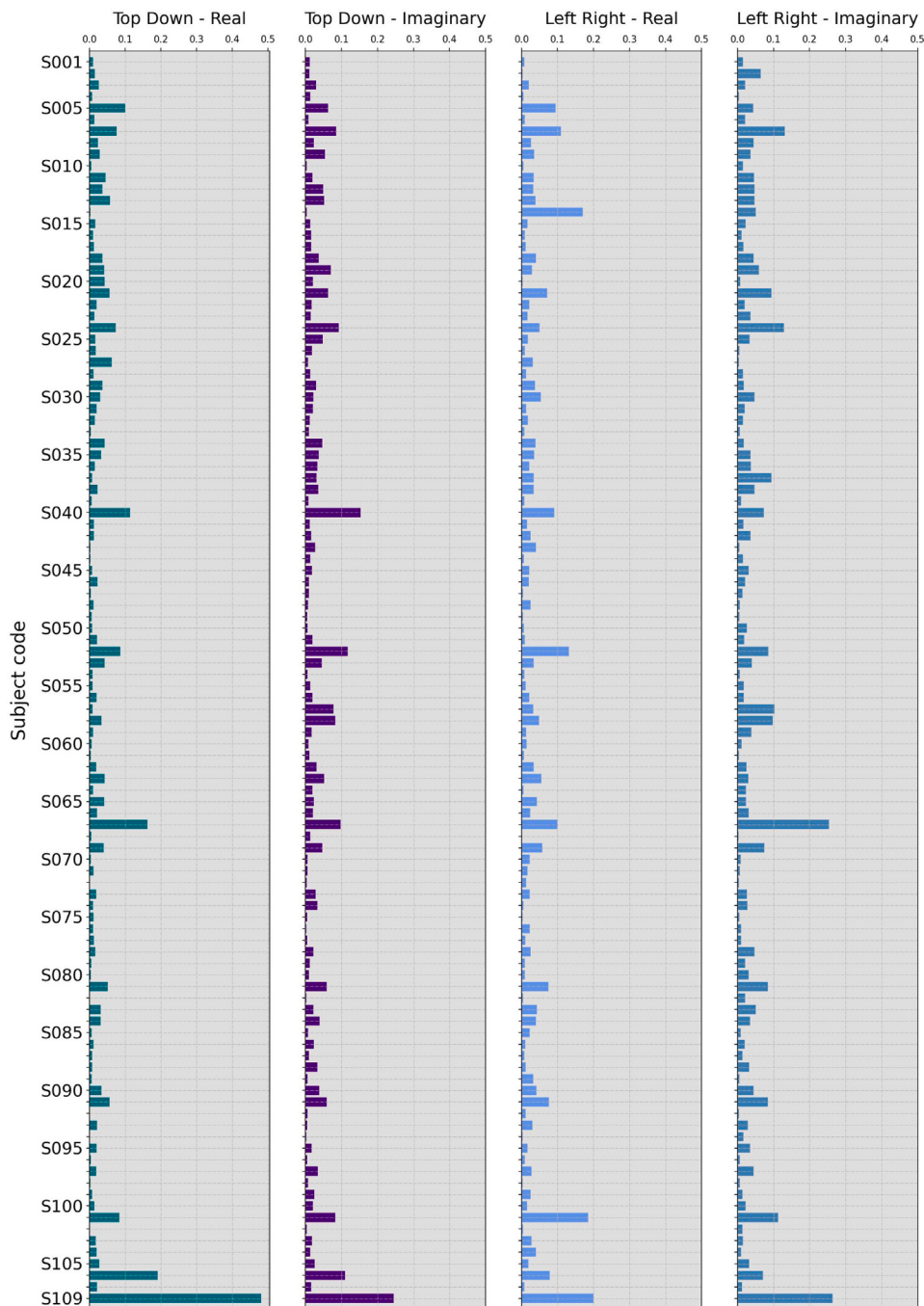
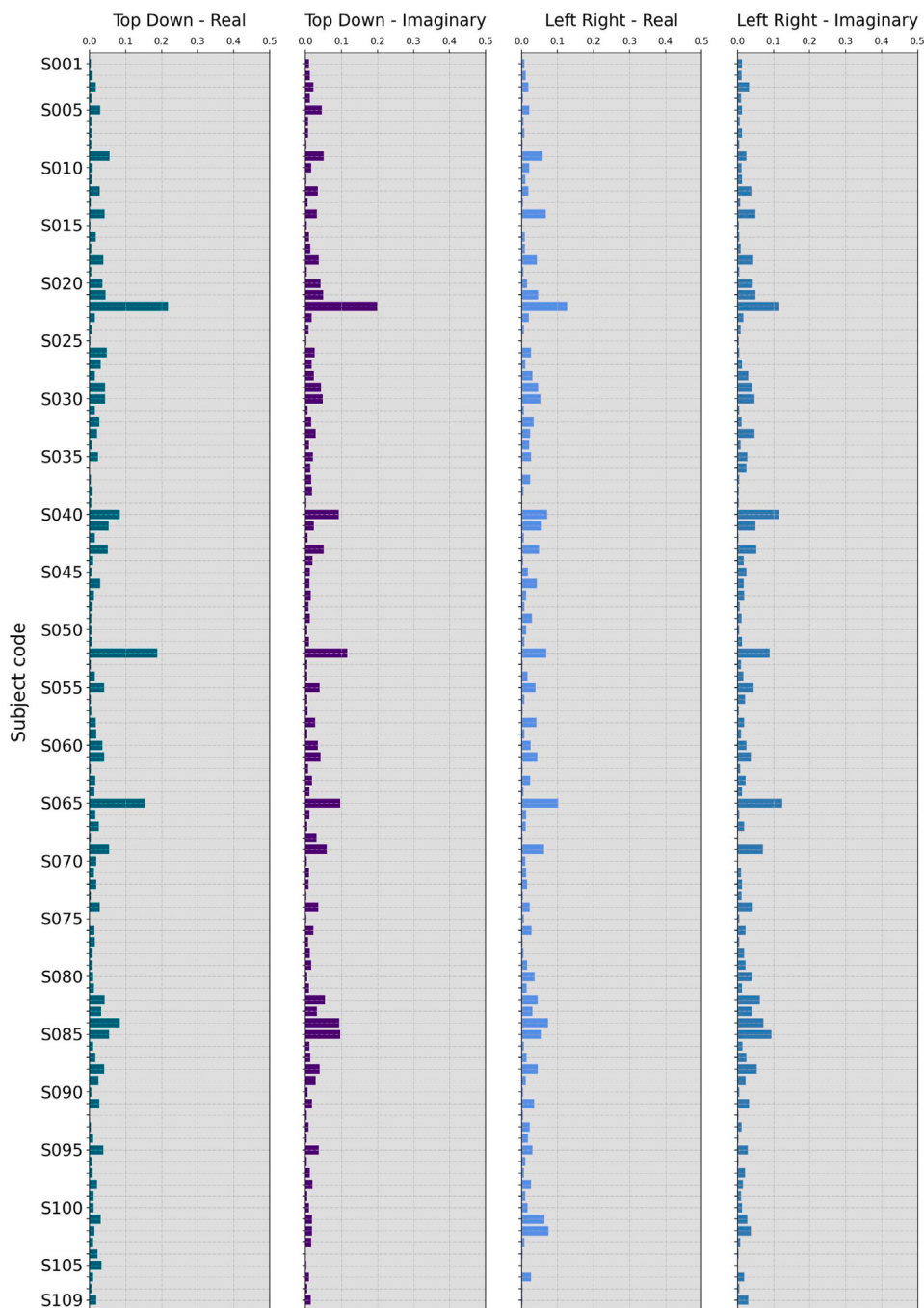
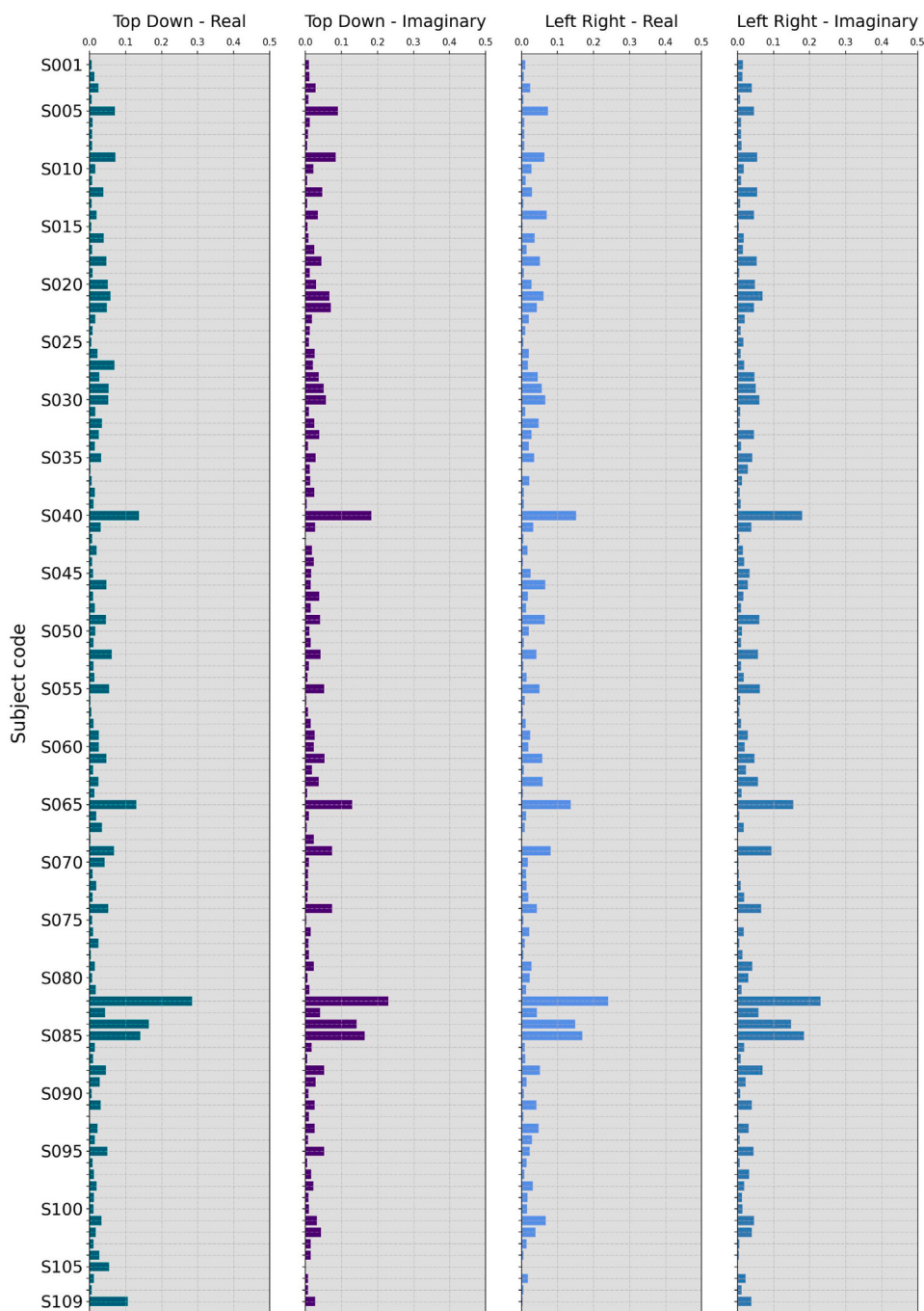


Fig. 10. MSE for the channel F_3 .

Fig. 11. MSE for the Channel F_6 .

Fig. 12. MSE for the Channel P_3 .

Fig. 13. MSE for the Channel P_6 .**CRediT authorship contribution statement**

Fernando Ferraz Ribeiro: Writing – original draft, Visualization, Software, Investigation. **Andréa de Almeida Brito:** Visualization, Resources, Methodology, Conceptualization. **Florêncio Mendes Oliveira Filho:** Writing – original draft, Visualization, Validation, Investigation, Formal analysis, Data curation. **Juan Alberto Leyva Cruz:** Writing – review & editing, Validation, Investigation, Formal analysis. **Gilney Figueira Zebende:** Writing – review & editing, Writing – original draft, Visualization, Validation, Supervision, Resources, Project administration, Methodology, Investigation, Formal analysis, Data curation, Conceptualization.

Declaration of competing interest

The authors declare that they have no known competing financial interests or personal relationships that could have appeared to influence the work reported in this paper.

Acknowledgments

G. F. Zebende and F. M. Oliveira Filho thanks the Brazilian agency CNPq (Conselho Nacional de Desenvolvimento Científico e Tecnológico), Brazil (Grants 310136/2020-2 and 150655/2022-3, respectively). We would also like to thank Paulo Murilo Castro de Oliveira, great statistical physicist (*in memoriam*).

Data availability

Data will be made available on request.

References

- [1] M. Tudor, L. Tudor, K.I. Tudor, Hans berger (1873-1941) - the history of electroencephalography, *Acta Medica Croatica* 59 (4) (2005) 307–313.
- [2] A. Biasiucci, B. Franceschiello, M.M. Murray, Electroencephalography, *Curr. Biol.* 29 (30) (2019) R80–R85.
- [3] G.F. Zebende, F.M. Oliveira-Filho, J.A. Leyva-Cruz, Auto-correlation in the motor/imaginary human EEG signals: A vision about the FDFA fluctuations, *PLoS One* 12 (9) (2017).
- [4] F.M. Oliveira Filho, J.A. Leyva Cruz, G.F. Zebende, Analysis of the EEG bio-signals during the reading task by DFA method, *Phys. A (ISSN: 0378-4371)* 525 (2019) 664–671.
- [5] V.B. Mesquita, F.M. Oliveira-Filho, P.C. Rodrigues, Detection of crossover points in detrended fluctuation analysis: An application to EEG signals of patients with epilepsy, *Bioinformatics* (2020) <http://dx.doi.org/10.1093/bioinformatics/btaa955>.
- [6] F. Oliveira Filho, F. Ribeiro, J.L. Cruz, A.N. de Castro, G. Zebende, Statistical study of the EEG in motor tasks (real and imaginary), *Phys. A (ISSN: 0378-4371)* (2023) 128802.
- [7] G. Zebende, A. da Silva Filho, Detrended multiple cross-correlation coefficient, *Phys. A* 510 (2018) 91–97.
- [8] G. Schalk, D.J. McFarland, T. Hinterberger, N. Birbaumer, J.E. Wolpaw, BCI2000: a general-purpose brain-computer interface (BCI) system, *IEEE Trans. Biomed. Eng.* 51 (6) (2004) 1034–1043.
- [9] C.K. Peng, S.V. Buldyrev, S. Havlin, M. Simons, H.E. Stanley, A.L. Goldberger, Mosaic organization of DNA nucleotides, *Phys. Rev. E* 49 (1994) 1685–1689.
- [10] B. Podobnik, Z.-Q. Jiang, W.-X. Zhou, H.E. Stanley, Statistical tests for power-law cross-correlated processes, *Phys. Rev. E* 84 (2011) 1–8.
- [11] J.C. Zhao, W.H. Dou, H.D. Ji, J. Wang, Detrended cross-correlation analysis of epilepsy electroencephalogram signals, *Adv. Mater. Res.* 765–767 (2013) 2664–2667.
- [12] Y. Chen, L. Cai, R. Wang, Z. Song, B. Deng, J. Wang, H. Yu, DCCA cross-correlation coefficients reveals the change of both synchronization and oscillation in EEG of alzheimer disease patients, *Phys. A* 490 (2018) 171–184.
- [13] G. Zebende, DCCA cross-correlation coefficient: Quantifying level of cross-correlation, *Phys. A* 390 (4) (2011) 614–618.
- [14] L. Kristoufek, Measuring cross-correlation between non-stationary series with DCCA coefficient, *Phys. A* 402 (2014) 291–298.
- [15] A.A. Brito, H.A. Araujo, G.F. Zebende, Detrended multiple cross-correlation coefficient applied to solar radiation, air temperature and relative humidity, *Sci. Rep.* 9 (2019) 19764, <http://dx.doi.org/10.1038/s41598-019-56114-6>.
- [16] A.M. da Silva Filho, G.F. Zebende, A.P.N. de Castro, E.F. Guedes, Statistical test for multiple detrended cross-correlation coefficient, *Phys. A* 562 (2021) 125285.
- [17] E.F. Guedes, A.M. da Silva Filho, G.F. Zebende, Detrended multiple cross-correlation coefficient with sliding windows approach, *Phys. A* 574 (2021) 125990.
- [18] E.F. Guedes, A.P.N. de Castro, A.M. da Silva Filho, G.F. Zebende, Δ DMC \times 2: A new approach to measure contagion effect on financial crisis, *Fluct. Noise Lett.* 21 (04) (2022) 2250026.
- [19] G.F. Zebende, L.C. Aguiar, P. Ferreira, E.F. Guedes, Statistical approach to study the relationship between stock market indexes by multiple DCCA cross-correlation coefficient, *Fluct. Noise Lett.* 21 (5) (2022) 2250045–2251314.